©Journal of Sports Science and Medicine (2009) **8,** 584-590
http://www.jssm.org

**Research article**

# Noninvasive determination of knee cartilage deformation during jumping

**Nenad Filipovic [1,3]✉, Radun Vulovic [1], Aleksandar Peulic [1], Radivoje Radakovic [1], Djordje Kosanic [2] and Branko Ristic [1,4]**

[1] Bioengineering Research and Development Center, BioIRC, [2] Sport Center "Mladost", [3] Faculty of Mechanical Engineering University of Kragujevac, [4] Medical Faculty Kragujevac, University of Kragujevac, Kragujevac, Serbia.

**Abstract**

The purpose of this investigation was to use a combination of image processing, force measurements and finite element modeling to calculate deformation of the knee cartilage during jumping. Professional athletes performed jumps analyzed using a force plate and high-speed video camera system. Image processing was performed on each frame of video using a color recognition algorithm. A simplified mass-spring-damper model was utilized for determination of global force and moment on the knee. Custom software for fitting the coupling characteristics was created. Simulated results were used as input data for the finite element calculation of cartilage deformation in the athlete's knee. Computer simulation data was compared with the average experimental ground reaction forces. The results show the three-dimensional mechanical deformation distribution inside the cartilage volume. A combination of the image recognition technology, force plate measurements and the finite element cartilage deformation in the knee may be used in the future as an effective noninvasive tool for prediction of injury during jumping.

**Key words:** Simulation, athletes, injury.

## Introduction

New video capture boards, automatic digitizing, real-time transformation, and filtering software have recently been developed. This allows for kinematic and kinetic data to be displayed simultaniously (Altmeyer et al., 1994; Ariel et al., 1997; Borelli, 1989). This data can be time-synchronized so that a researcher, coach, and athlete could effectively evaluate athletic performance under various competitive conditions. It may also be of assistance for making adjustments to training (Braune et al., 1987; Finch et al., 1998; Plagenhoef, 1968). Tendon injuries occur often in sports (Josza and Kannus, 1997), especially in explosive sports where a high demand of force, speed and power are utilized for optimal performance.

Athletes are repeatedly subjected to continuously high stress during exercise which makes the bone tendon junction, being the weakest point, susceptible to lesion. Cumulative microtrauma may occur which weakens collagen cross-linking and finally results in mucoid degeneration of the tendon (Khan et al., 1998). As a result noninvasive determination of cartilage deformation in the knee may be very useful tool for prediction of knee injury. In the current investigation, video analysis of images, together with the force plate measurement, were utilized to determine deformation of the cartilage in the knee.

Video acquisition and parsing sequences of images significantly influences the performance of tracking algorithms. Careful planning of image acquisition is crucial for the success of the proposed system. Motion tracking of small objects can be quite difficult and depends on many parameters with special attention on environmental conditions and the type of video acquisition system. Although various tracking algorithms have been developed in the past, their robustness has not been clearly described in the literature. The existing methods can be roughly classified as high-tech hardware based, and algorithm based. In the first group, high-tech hardware is used, i.e. high quality video, multiple high-tech cameras and lenses, powerful high-end computers, best lighting etc. In such a case, applied algorithms are not very sophisticated. Often a blob tracker is sufficient (Pingali et al, 1998, 2000). The primary issue is to set-up and coordinate multiple cameras, or to visualize results of motion tracking, for example in a 3-D virtual environment (Pingali et al, 1998, 2000). However, special and very sophisticated algorithms that are able to resolve the task of compensation of demerits must be employed. In this paper, a method is proposed that compromises between two previously described methods. One utilized only a high-speed camera while our motion tracking software is based on a moving seed point algorithm. Using a high-speed camera for complex kinematics calculations in the motion tracking was avoided. A few similar advanced algorithms were able to address the issue when various experimental conditions are implemented.

In this study a combined image processing tracking algorithm was used in order to measure kinematics and dynamics of athletes jumping on a force plate, together with numerical calculation of cartilage deformation in the knee. In the following section the procedure for force measurement, the basic algorithm for image tracking the object, as well as numerical finite element methods for cartilage deformation is explained.

## Methods

### Force measurement

Knee motion involves a series of three rotations (flexion/extension, abduction/adduction, and internal/external rotations) and three translations (anterior/posterior, superior/inferior, and medial/lateral translations). Our first goal was to develop a computer vision system for motion tracking and analysis of the force measurement of athlete's knees during jumping. These recorded impact

Received: 20 June 2009 / Accepted: 11 September 2009 / Published (online): 01 December 2009

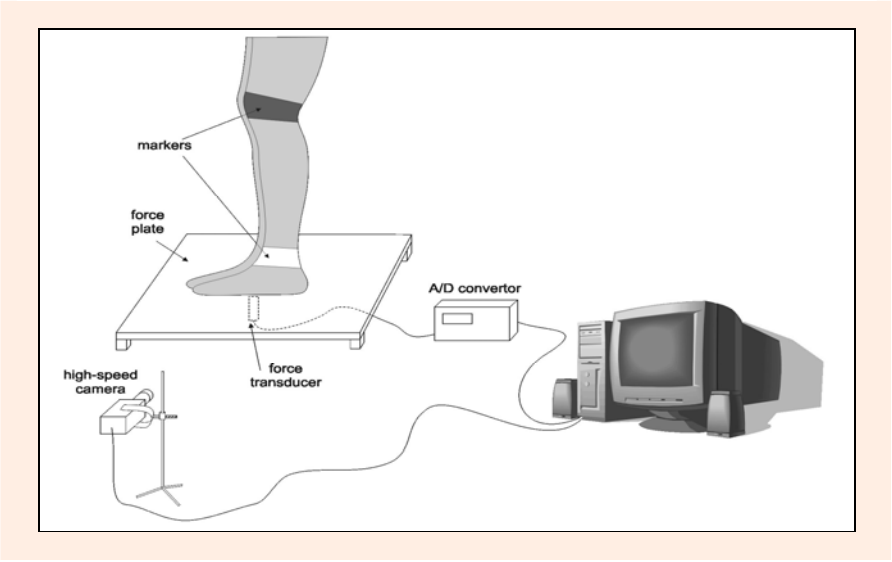


**Figure 1.** **Setup equipment for experimental investigation of jumping impact force and knee force and moment.**

forces were used to calculate the internal forces in the ankle and knee. For this purpose we designed a separate device, a so called "force plate," with force transducer mounted on it. The force measurements were recorded completely in parallel with video analysis which was controlled with a specific in-house software system (Figure 1). After acquisition of the experimental results, we used our video and image processing software for analysis and preparation of data into numerical calculations. The measurement results were determined for the ankle and knee separately in the form of triplet values: x-coordinate, y-coordinate and vertical resistance force F.

For each individual jump, the following variables were measured: a) frame-rate, b) total time of experiment, c) 2D coordinates of ankle and knee for every frame, d) corresponding forces measured on the force plate for each contact, e) number of jumps and f) maximal velocity gained at the moment of landing. The primary goal of our experiment was to simultaneously record video and force plate data. High-speed (Basler A602fc) cameras were used to record for a duration of 10 seconds. A corresponding AVI file format of approximately 1.2 GB was saved, with the following properties: 100 fps, 656x490 px, YUV 4:2:2 (16 bits/pixel avg.). At the same time (in parallel), we were recording measurements from the force transducer through a serial port. In each case, system time was recorded for synchronization of our measurements.

Additionally, this phase also included determination of some parameters that were needed for the following numerical calculations. These were: a) separation of individual jumps, ie. determination of the start and end jump times, b) calculation of the velocities of jump landings, c) measurement of the force generated in the contact area, and d) filtering of the force measurements due to inertia of the force plate itself. To fulfill these requirements, we ascertained some criteria. They were mostly influenced by our subjective visual impressions and conclusions about the jumps and they were in accordance with changes in the force measurements. Nine phases of the jump were defined: 1) rest, 2) preparation for jump, 3) rebound, 4) lateness in air, 5) fall, 6) toe landing, 7) heel landing, 8) preparation for rest, and 9) rest. The second criterion was related to determination of landing velocity during the jump. There were horizontal and vertical components of velocity during the fall. At the moment when the athlete landed (6$^{th}$ phase of the jump) velocity gained its maximum value, which was used as a parameter for subsequent numerical calculations. This value can be determined by integrating velocities between subsequent frames, starting with the frame where this value was 0. The starting frame for this calculation was considered a frame at the very end of the 4$^{th}$ phase of the jump, or the very first frame of the 5$^{th}$ phase of the jump. As the acceleration during the fall was approximately constant, maximum velocity at the time the athlete touched the force plate was calculated using the next formula:

$$v_{max}^{px} = \sqrt{v_{max\_x}^2 + v_{max\_y}^2} = \frac{\sqrt{(x_m - x_n)^2 + (y_m - y_n)^2}}{m - n} \quad (1)$$

Were n and m represented indexes of the starting and ending frames, respectively. In the same sense, x and y values were coordinates of the ankle. Velocity according to the equation (1) was expressed in [pixels/frame count]. To express maximal velocity in ISO units [m/s], $v_{max}^{px}$ must be multiplied by the coefficient K:

$$v_{max} = v_{max}^{px} \cdot K = v_{max}^{px} \cdot \frac{0.68}{230} \cdot fps \quad (2)$$

Where 0.68 meters was represented by 230 pixels at image frames.

## Proposed image processing motion tracking algorithm

In this section we describe the problem of tracking movable objects in a movie file recorded during the experimental measurements. The aim was not to develop software that would be used for real-time image processing, but to develop an application that would be simple, reliable, precise, extensible and yet powerful enough to fit the requirements and challenges of our experiment.

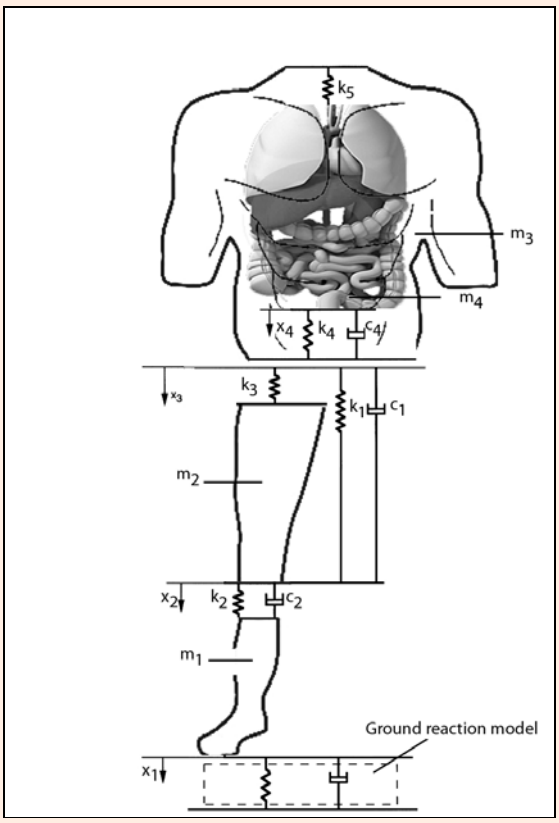


**Figure 2. A simplified spring-damper-mass model used in the computer simulation. The components of dynamics system presented are: lower body rigid mass (*m*1) and wobbling mass (*m*2), upper body rigid mass (*m*3) and wobbling mass (*m*4), compressive spring (*k*1) and damper (*c*1) that connect the upper and lower rigid bodies, spring (*k*3) and spring}damper unit (*k*2, *c*2) connecting the lower wobbling mass to the upper and lower rigid bodies, spring (*k*5) and spring}damper unit (*k*4, *c*4) connecting the upper wobbling mass to the upper rigid mass (Liu et al., 1998).**

Tracking of movable objects has always been a challenging task without a single, universal solution. Among other things, it is heavily dependent on the quality of the video material, i.e. it indirectly depends on image acquisition hardware and overall environmental recording conditions. Keeping that in mind, we decided to make a compromise between hardware and software solutions. For our experiment we used a high-speed (Basler A602fc) color camera, with 100 fps and 656x490 pixels resolution. Using this high frame rate, we avoided having to develop complex algorithm for motion tracking. In essence, there are two basic algorithms for motion tracking: an area based approach and a differential approach (Mark et al., 2002). These are based on so called "optical flow", where image features in subsequent frames are related to each other to some degree. In fact, "motion can be characterized as a collection of displacements in the image plane" (Mark et al., 2002). The first method focused on feature (e.g. pixels) similarities between intensities in the image regions. The second method dealt with observation of the differential changes in the pixel values. Our method was simpler and quite different and it was based on finding a new "seed point". We will describe how to define the initial seed point and select the area of the object which needs to be tracked, as well as how to start the whole tracking process.

In order to track movements of the ankle and knee we decided to put colored markers on them such that their color distinguishes them from a uniform colored background. In that way we avoided steps related to image enhancements, as we already had objects of distinct colors, so tracking can be performed only on that feature. In this case, two methods for motion tracking were imposed. The first method was used to track a single colored object from frame-to-frame with regard only to its position and color features. The second method assumed definition of AOI (Area Of Interest) of the image and scanning for a given color. Due to artifacts in the image (e.g. caused by image compression algorithm), the first method was preferred. It was more precise than the second method and is described in the following text.

The initial step in our motion tracking algorithm was manual detection of a seed point and definition of the upper and lower tolerances for the color components (R,G,B) of the seed point. By defining tolerances for the color components we actually defined the selection area around the seed point, which was composed of pixels that share similar features (color), i.e. pixels whose color was inside tolerances defined for a given seed point. An algorithm was used to actually define the selection area (A) which was based on neighborhood operations and used a stack as storage for the connected components (i.e pixels). It was obvious that this algorithm may be considered as a sort of float-fill (propagation) algorithm (Glassner, 2001).

## Spring-damper-mass model

A simplified spring-damper-mass model which was used in this study is shown in Figure 2. It consists of four masses. The upper body was modeled using two masses, one representing its rigid mass, $m_3$, and the other representing its wobbling mass, $m_4$. The thigh, leg and foot of the supporting leg were modeled using two masses, one representing its rigid mass, $m_1$, and the other representing its wobbling mass, $m_2$. The total body mass was obtained from the subject. In the following system of equations (Equation 3) a dynamics system is described (Liu et al, 1998) and it was used for the calculation of total force and the moment of the cartilage in the knee during the jump.

$$\begin{aligned}
&m_1\ddot{x}_1 + k_1(x_1 - x_3) + k_2(x_1 - x_2) + c_1(\dot{x}_1 - \dot{x}_3) + c_2(\dot{x}_1 - \dot{x}_2) = m_1 g - F_g \\
&m_2\ddot{x}_2 - k_2(x_1 - x_2) + k_3(x_2 - x_3) - c_2(\dot{x}_1 - \dot{x}_2) = m_2 g \\
&m_3\ddot{x}_3 - k_1(x_1 - x_3) - k_3(x_2 - x_3) + \\
&(k_4 + k_5)(x_3 - x_4) - c_1(\dot{x}_1 - \dot{x}_3) + c_4(\dot{x}_3 - \dot{x}_4) = m_3 g \\
&m_4\ddot{x}_4 - (k_4 + k_5)(x_3 - x_4) - c_4(\dot{x}_3 - \dot{x}_4) = m_4 g
\end{aligned} \tag{3}$$

In Equation 3, $m_1$ was the lower body rigid mass and $m_2$ was the wobbling mass, $m_3$ was the upper body rigid mass and $m_4$ was the wobbling mass, $k_1$ was the compressive spring and $c_1$ was the damper that connected the upper and lower rigid bodies, $k_3$ was the spring and $k_2$-$c_2$ was the spring-damper unit which connected the lower wobbling mass to the upper and lower rigid bodies, $k_5$ was the

spring and $k_4$-$c_4$ was the spring-damper unit which connected the upper wobbling mass to the upper rigid mass (Liu et al, 1998 ). $F_g$ was the vertical contact force which was defined as $F_g = A_c\left[ax_1^b + cx_1^d v_1^e\right]$, and $A_c$, $a,b,c,d,e$ were the parameters for the ground reaction model which defined the deformation of the shoes during jumping. Some of the different parameters for soft and hard shoes are shown in Table 1.

**Table 1. Parameters for ground reaction model.**

| | $a$ | $b$ | $c$ | $d$ | $e$ |
|---|---|---|---|---|---|
| **Soft shoe** | $1 \times 10^6$ | 1.56 | $2 \times 10^4$ | 0.73 | 1.0 |
| **Hard shoe** | $1 \times 10^6$ | 1.38 | $2 \times 10^4$ | 0.75 | 1.0 |

## Finite element method for numerical calculation

Cartilage inside the knee was considered as a porous deformable body filled with fluid, occupying the whole pore volume. The physical quantities for this analysis were: the displacement of solid **u**, relative fluid velocity with respect to the solid (Darcy's velocity) **q**, fluid pressure p, swelling pressure $p_c$, and electrical potential $\phi$. The governing equations for the coupled problem are described as following. First, we considered the solid equilibrium equation,

$$(1-n)\mathbf{L}^T\boldsymbol{\sigma}_s + (1-n)\rho_s\mathbf{b} + \mathbf{k}^{-1}n\mathbf{q} - (1-n)\rho_s\ddot{\mathbf{u}} = 0 \qquad (4)$$

where $\boldsymbol{\sigma}_s$ was the stress in the solid phase, n was porosity, **k** was the permeability matrix, $\rho_s$ was the density of the solid, **b** was body force per unit mass, **q** was relative velocity of the fluid, and $\ddot{\mathbf{u}}$ was acceleration of the solid material. The operator $\mathbf{L}^T$ was

$$\mathbf{L}^T = \begin{bmatrix} \frac{\partial}{\partial x_1} & 0 & 0 & \frac{\partial}{\partial x_2} & 0 & \frac{\partial}{\partial x_3} \\ 0 & \frac{\partial}{\partial x_2} & 0 & \frac{\partial}{\partial x_1} & \frac{\partial}{\partial x_3} & 0 \\ 0 & 0 & \frac{\partial}{\partial x_3} & 0 & \frac{\partial}{\partial x_2} & \frac{\partial}{\partial x_1} \end{bmatrix} \qquad (5)$$

The equilibrium equation of the fluid phase (no electrokinetic coupling) was

$$-n\nabla p + n\rho_f\mathbf{b} - \mathbf{k}^{-1}n\mathbf{q} - n\rho_f\dot{\mathbf{v}}_f = \mathbf{0} \qquad (6)$$

where p was pore fluid pressure, $\rho_f$ was fluid density and $\dot{\mathbf{v}}_f$ was fluid acceleration. This equation is also known as the generalized Darcy's law. Both equilibrium equations were written per unit volume of the mixture. Combining Equations (4) and (6) we obtained

$$\mathbf{L}^T\sigma + \rho\mathbf{b} - \rho\ddot{\mathbf{u}} - \rho_f\dot{\mathbf{q}} = \mathbf{0} \qquad (7)$$

where $\boldsymbol{\sigma}$ was the total stress which can be expressed in terms of $\boldsymbol{\sigma}_s$ and p, as

$$\boldsymbol{\sigma} = (1-n)\,\boldsymbol{\sigma}_s - n\mathbf{m}p \qquad (8)$$

and $\rho=(1-n)\rho_s+n\rho_f$ was the mixture density. Here **m** was a constant vector defined as $\mathbf{m}^T=\{1\ 1\ 1\ 0\ 0\ 0\}$ to indicate that the pressure component contributes to the normal stresses only. We had to also take into account that the pressure has a positive sign in compression, while tensional stresses and strains were considered positive as well. In the following analysis we employed the effective stress, $\boldsymbol{\sigma}'$, defined as

$$\boldsymbol{\sigma}' = \boldsymbol{\sigma} + \mathbf{m}p \qquad (9)$$

which was relevant for the constitutive relations of the solid. Using the definition of relative velocity **q** as the volume of the fluid passing in a unit time through a unit area of the mixture (Darcy's velocity),

$$\mathbf{q} = n\left(\mathbf{v}_f - \dot{\mathbf{u}}\right) \qquad (10)$$

we transformed (6) into

$$-\nabla p + \rho_f\mathbf{b} - \mathbf{k}^{-1}\mathbf{q} - \rho_f\ddot{\mathbf{u}} - \frac{\rho_f}{n}\dot{\mathbf{q}} = \mathbf{0} \qquad (11)$$

The final continuity equation using the elastic constitutive law and fluid incompressibility was given in the form (Kojic et al, 2001)

$$\nabla^T\mathbf{q} + \left(\mathbf{m}^T - \frac{\mathbf{m}^T\mathbf{C}^E}{3K_s}\right)\dot{\mathbf{e}} + \left(\frac{1-n}{K_s} + \frac{n}{K_f} - \frac{\mathbf{m}^T\mathbf{C}^E\mathbf{m}}{9K_s^{\,2}}\right)\dot{p} = 0 \qquad (12)$$

The resulting FE system of equations was solved incrementally (Kojic et al, 2001), with time step $\Delta t$. We imposed the condition that the balance equations are satisfied at the end of each time step ($t+\Delta t$). Hence, we derived the following system of equations

$$\begin{bmatrix} \mathbf{m}_{uu} & 0 & 0 & 0 \\ 0 & 0 & 0 & 0 \\ \mathbf{m}_{qu} & 0 & 0 & 0 \\ 0 & 0 & 0 & 0 \end{bmatrix} \begin{Bmatrix} {}^{t+\Delta t}\ddot{\underline{\mathbf{u}}} \\ {}^{t+\Delta t}\ddot{\underline{\mathbf{p}}} \\ {}^{t+\Delta t}\ddot{\underline{\mathbf{q}}} \\ {}^{t+\Delta t}\ddot{\underline{\phi}} \end{Bmatrix} + \begin{bmatrix} 0 & 0 & \mathbf{c}_{uq} & 0 \\ \mathbf{c}_{pu} & \mathbf{c}_{pp} & 0 & 0 \\ 0 & 0 & \mathbf{c}_{qq} & 0 \\ 0 & 0 & 0 & 0 \end{bmatrix} \begin{Bmatrix} {}^{t+\Delta t}\dot{\underline{\mathbf{u}}} \\ {}^{t+\Delta t}\dot{\underline{\mathbf{p}}} \\ {}^{t+\Delta t}\dot{\underline{\mathbf{q}}} \\ {}^{t+\Delta t}\dot{\underline{\phi}} \end{Bmatrix} \qquad (13)$$

$$+ \begin{bmatrix} \mathbf{k}_{uu} & \mathbf{k}_{up} & 0 & 0 \\ 0 & 0 & \mathbf{k}_{pq} & 0 \\ 0 & \mathbf{k}_{qp} & \mathbf{k}_{qq} & \mathbf{k}_{q\phi} \\ 0 & \mathbf{k}_{\phi p} & 0 & \mathbf{k}_{\phi\phi} \end{bmatrix} \begin{Bmatrix} \Delta\underline{\mathbf{u}} \\ \Delta\underline{\mathbf{p}} \\ \Delta\underline{\mathbf{q}} \\ \Delta\underline{\phi} \end{Bmatrix} = \begin{Bmatrix} {}^{t+\Delta t}\mathbf{f}_u \\ {}^{t+\Delta t}\mathbf{f}_p \\ {}^{t+\Delta t}\mathbf{f}_q \\ {}^{t+\Delta t}\mathbf{f}_\phi \end{Bmatrix}$$

Where $f_u$, $f_p$, $f_q$ and $f_\Phi$ were forces in the balance equations for displacement, pressure, fluid velocity and electrical potential respectively, and $m_{uu}$ and $m_{qu}$ were mass terms in mass matrix.

## Results

The goal of this study was to calculate cartilage deformation in the knee joint based on a subject knee model andbiomechanical analysis of jumping. The overall forces on the knee joint were presented in Figure 3. Although there are many different forces which act on the knee, for simplicity we considered only one dimensional force determined from the dynamics system in Equation 3.

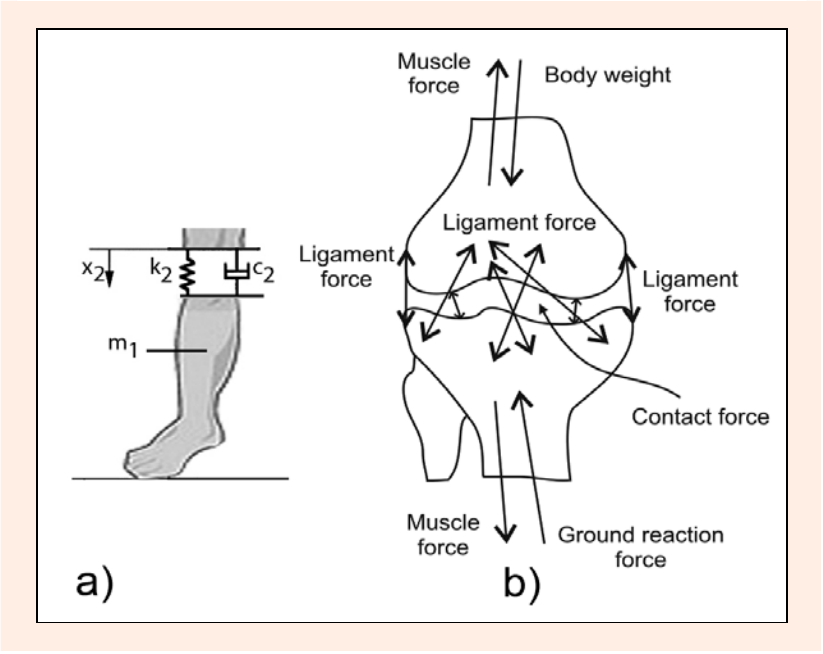


**Figure 3. A schematic force approximation on the knee joint. a) Dynamics system of knee deformation during jumping; b) Description of forces inside a knee joint.**

The dialog menu of developed software for the capture motion of the subject is presented in Figure 4.

Drawing a line along the lower limb of the subject in Figure 4 presented a tracking of rigid lower body with two points or joints. The upper joint corresponded to a knee motion and the force applied to this point was of particular interest for cartilage deformation. The force which was measured from the force plate is shown in figure 5. Using these experimental results we calculated the force and moment on the cartilage in the knee as it is described in the second section method. The knee joint was analyzed as an electrokinetic transduction in charged, homogenous, isotropic, hydrated material. In the analysis we first used the material constants from Frank et al., (1987a; 1987b). After that, we fitted values of the material constants to experimental data by employing our numerical solutions. The results of fitting were given in figure 6 and basic fitted parameters were shown in Table 2.

Following the approach of Frank et al., 1987a; Frank et al., 1987b, the fluid and the solid domain were assumed to be incompressible, and the tissue compression was taken as a constant. The Young modulus of elasticity was $E = 4.5 \times 10^3$ [N/m$^2$] and $K_f = 2.2 \times 10^9$. The average peak force was detemined from the ground reaction force measured on the force plate (Figures 5 and 6) and solving a one-dimensional system of equations (Equation 3). The result for cartilage deformation for the average peak force of 166 N is presented in Figure 7.


**Figure 4. 3D capture imaging and the force plate measurements during sportsman's jumping.**

**Table 2. Fitted parameters of dynamics system.**

| Mass | $m_1$ =7 kg | $m_2$ = 6 kg | $m_3$ = 14 kg | $m_4$ = 45 kg | |
|---|---|---|---|---|---|
| Stiffness | $k_1$ = 6000 N/m | $k_2$ = 5000 N/m | $k_3$ = 9000 N/m | $k_4$ = 9000 N/m | $k_5$ = 16000 N/m |
| Damping | $c_1$ = 250 kg/s | $c_2$ = 600 kg/s | $c_4$ = 1700 kg/s | | |

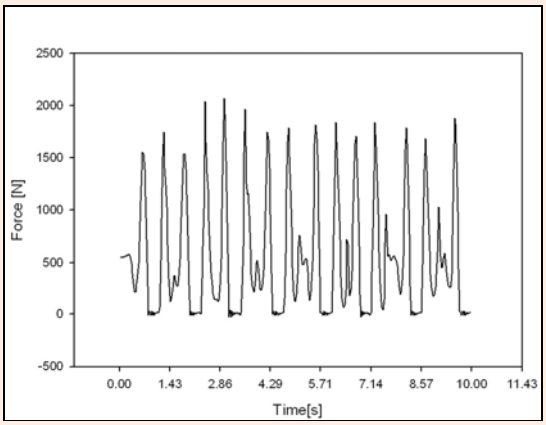


**Figure 5. Force vs time during jumping testing phase.**

## Discussion

The range of estimated peak force corresponded to some previous study for the vertical force inside the human knee (Lee et al 2004). The one-dimensional approximation of the dynamic model in equation 3 seemed to be reasonable. The geometrical data for the cartilage model were parameterized according to the knee model from the literature (Fernandez and Pandy 2006). The initial results for cartilage deformation were also in the range of some previous computational study (Bei and Fregly 2004). This was determined to be a good starting point for noninvasive determination of the cartilage stress and deformation as well as other parts of the knee model.

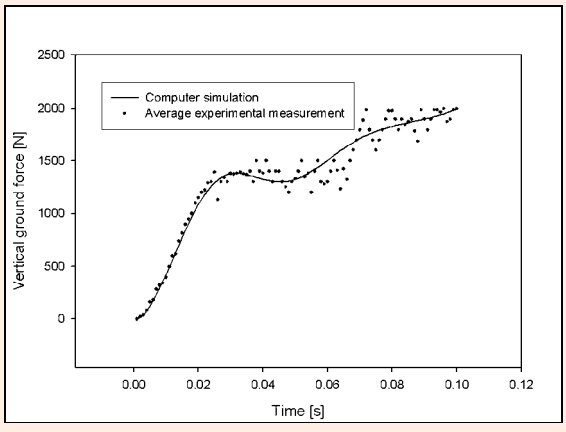


**Figure 6. Fitting of dynamics parameters for the ground contact force *Fg* (see Eq.3).**

## Conclusion

We have presented a combined image processing tracking algorithm for measurement of kinematics and dynamics of jumping on a force plate. A simplified algorithm of the spring-damper-mass model for determination of force and moment on the cartilage inside the knee was developed. Three dimensional finite element calculation of cartilage deformation during knee motion was implemented.

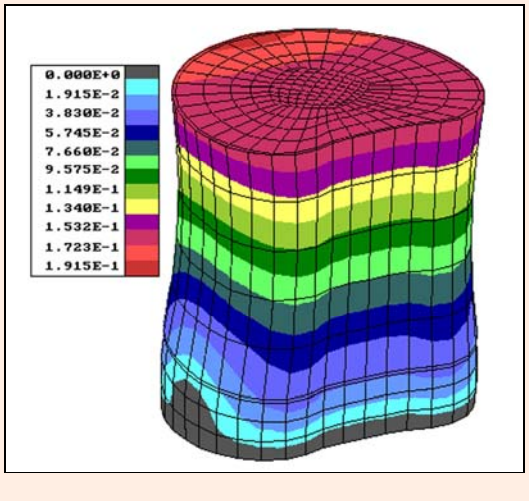


**Figure 7. Cartilage deformation for a peak force = 166 N during jumping on the force plate. The units in the palette color for deformation are "cm".**

These experimental and computational techniques could be a good platform for future athlete testing. By using this methodology coaches may effectively evaluate athletic performance under various competitive conditions and possibly avoid sports injuries during training. A next step would be to include the neuromuscular control of human jumping. Also we might consider the causal mechanism of jumper's knee in sport and possible risk factors in order to better understand them.

## Acknowledgments

This research was supported by Ministry of Science of Serbia, TR12007, OI144028.

## References

Altmeyer, L., Bartonietz, K. and Krieger, D. (1994) Technique and training: the discus throw. *Track & Field Quarterly Review* **94(3),** 33-34.

Ariel, G., Finch, A. and Penny, A. (1997) Biomechanical analysis of discus throwing at the 1996 Atlanta Olympic Games. *Biomechanics in Sports XV*. 365-371.

Borelli, K.D. (1989) *De motu animalium.pais prima* 1680. Springer Verlag, Berlin.

Braune, W. and Fischer, O. (1987) *The human gait*. Springer Verlag, Berlin.

Fernandez, J.W. and Pandy, M.G. (2006) Integrating modelling and experiments to assess dynamic musculoskeletal function in humans. *Experimental Physiology* **91,** 371–382.

Finch, A., Ariel, G. and Penny, A. (1998) Kinematic comparison of the best and worst of the top men's discus performers at the 1996 Atlanta Olympic Games. *International Symposium on Biomechanics in Sports* **I,** 93-96.

Frank, E.H. and Grodzinsky, AJ. (1987a) Cartilage electromechanics-I. Electrokinetic transduction and the effects of electrolyte pH and ionic strength. *Journal of Biomechanics* **20,** 615-627.

Frank, E.H. and Grodzinsky, AJ. (1987b) Cartilage electromechanics-II.

A continuum model of cartilage electrokinetics and correlation with experiments. *Journal of Biomechanic* **20,** 629-639.
Glassner, A. (2001) "Fill 'Er Up!". *IEEE Computer Graphics and Applications*. **21(1),** 78-85.
Jósza, L. and Kannus, P. (1997) Human tendons. Champaign, IL: Human Kinetics. 576.
Khan, K.M., Maffulli, N., Coleman, B.D., Cook, J.L. Taunton, J.E. (1998) Patellar tendinopathy: some aspects of basic science and clinical management. *British Journal of Sports Medicine* **32,** 346-355.
Kojic, M., Filipovic, N., Mijailovic, S. (2001) A large strain finite element analysis of cartilage deformation with electrokinetic coupling. *Computer Methods in Applied Mechanics and Engineering* **190,** 2447-2464.
Liu, W., Benno, M. and Nigg, A. (1998) Mechanical model to determine the influence of masses and mass distribution on the impact force during running. *Journal of Biomechanics* **33,** 219-224.
Mark, S., Nixon, Alberto, S. Aguado, (2002) *Feature Extraction and Image Processing.* Newnes.
Pingali, G.S., Jean, Y. and Carlbom, I. (1998) Real time tracking for enhanced tennis broadcasts. In: *Proceedings of the IEEE Computer Society Conference on Computer Vision and Pattern Recognition.* IEEE Computer Society. 260-265.
Pingali, G.S. Opalach, A. and Jean, Y. (2000) Ball tracking and virtual replays for innovative tennis broadcasts. *IEEE International Conference on Pattern Recognition* **4,** 152-156.
Plagenhoef, S. (1968) Computer programs for obtaining kinetic data on human movement. *Journal of Biomechanics* **1,** 221-234.
Lee, W., Zhang, M., Jia, X.,Cheung, J.. (2004) Finite Element Modeling of the Contact Interface Between Trans-Tibial Residual Limb and Prosthetic Socket. *Medical Engineering & Physics* **26(8),** 655-662.
Bei, Y. and Fregly, B. (2004) Multibody dynamic simulation of knee contact mechanics. *Medical Engineering & Physics* **26(9),** 777-789.

## Key points

- Even there are many existing mathematical models of force distribution during running or jumping (Liu et al, 1998), to our knowledge there is no interdisciplinary approach where imaging processing, finite element modeling and experimental force plate system are employed.
- The aim is to explore noninvasive deformation in the knee cartilage during athlete's jumping on the force plate.
- An original image algorithms and software were developed as well as complex mathematical models using high-performance computational power of finite element modeling together with one-dimensional dynamics model.
- The initial results showed cartilage deformation in the knee and future research will be focused on the methodology and more precisely determination of the stress and strain distribution in the knee cartilage during training phase of sportsman.

✉ **Nenad Filipovic**
Faculty of Mechanical Engineering, University of Kragujevac, Sestre Janjica 6, 34000 Kragujevac, Serbia

## AUTHORS BIOGRAPHY

**Nenad FILIPOVIC**
**Employment**
Faculty of Mechanical Engineering, University of Kragujevac, Sestre Janjica 6, 34000 Kragujevac
**Degree**
PhD
**Research interests**
Biomechanics, computer simulation, virtual human physiology
**E-mail:** fica@kg.ac.rs

**Radun VULOVIC**
**Employment**
Bioengineering Research and Development Center, BioIRC, Kragujevac, Serbia
**Degree**
MSc
**Research interests**
Image processing, computer science, java programming
**E-mail:** radun@kg.ac.rs

**Aleksandar PEULIC**
**Employment**
Bioengineering Research and Development Center, BioIRC, Kragujevac, Serbia
**Degree**
PhD
**Research interests**
Hardware, measurement equipment, automatic control
**E-mail:** apeulic@sbb.rs

**Radivoje RADAKOVIC**
**Employment**
Bioengineering Research and Development Center, BioIRC, Kragujevac, Serbia
**Degree**
MSc
**Research interests**
Sports training, coaching, conditional training
**E-mail:** dididi@yahoo.com

**Djordje KOSANIC**
**Employment**
Sports Center „Mladost", Kragujevac, Serbia
**Degree**
MSc candidate
**Research interests**
Sports training, biomechanics, sports engineering
**E-mail:** dididi@yahoo.com

**Branko RISTIC**
**Employment**
Medical Faculty Kragujevac, University of Kragujevac, Kragujevac, Serbia
**Degree**
PhD
**Research interests**
Sports and medicine, orthopedic biomechanics, sports biomechanics
**E-mail:** fica@kg.ac.rs